Osteoinductivity of nanostructured hydroxyapatite-functionalized gelatin modulated by human and endogenous mesenchymal stromal cells

06 October 2024

Osteoinductivity of nanostructured hydroxyapatite-functionalized gelatin modulated by human and endogenous mesenchymal stromal cells

Elena Della Bella [iD],[1,2] Annapaola Parrilli [iD],[3] Adriana Bigi,[4] Silvia Panzavolta,[4] Sofia Amadori,[4] Gianluca Giavaresi,[1] Lucia Martini,[1] Veronica Borsari,[1] Milena Fini[1]

[1]Laboratory of Preclinical and Surgical Studies, Rizzoli Orthopaedic Institute, via di Barbiano 1/10, 40136 Bologna, Italy
[2]Department of Medical and Surgical Sciences, University of Bologna, via G. Massarenti 9, 40138 Bologna, Italy
[3]Laboratory of Biocompatibility, Technological Innovations, and Advanced Therapies (BITTA), Rizzoli RIT Department, Rizzoli Orthopaedic Institute, via di Barbiano 1/10, 40136 Bologna, Italy
[4]Department of Chemistry "G. Ciamician", University of Bologna, via Selmi 2, 40126 Bologna, Italy

Abstract: The demand of new strategies for the induction of bone regeneration is continuously increasing. Biomimetic porous gelatin-nanocrystalline hydroxyapatite scaffolds with tailored properties were previously developed, showing a positive response in terms of cell adhesion, proliferation, and differentiation. In the present paper, we focused on their osteoinductive properties. The effect of scaffolds on osteogenic differentiation of human mesenchymal stromal cells (hMSCs) was investigated *in vitro*. hMSCs were seeded on GEL (type A gelatin) and GEL containing 10 wt% hydroxyapatite (GEL-HA) and cultured in osteogenic medium. Results showed that GEL and GEL-HA10 sustained hMSC differentiation, with an increased ALP activity and a higher expression of bone specific genes. The osteoinductive ability of these scaffolds was then studied *in vivo* in a heterotopic bone formation model in nude mice. The influence of hMSCs within the implants was examined as well. Both GEL and GEL-HA10 scaffolds mineralized when implanted without hMSCs. On the contrary, the presence of hMSC abolished or reduced mineralization of GEL and GEL-HA10 scaffolds. However, we could observe a species-specific response to the presence of HA, which stimulated osteogenic differentiation of human cells only. In conclusion, the scaffolds showed promising osteoinductive properties and may be suitable for use in confined critical defects. © 2017 Wiley Periodicals, Inc. J Biomed Mater Res Part A: 00B:000–000, 2017.

Key Words: osteoinduction, human bone marrow mesenchymal stromal cells, ectopic bone formation, gelatin-based scaffolds, bone tissue engineering, hydroxyapatite

How to cite this article: Della Bella E, Parrilli A, Bigi A, Panzavolta S, Amadori S, Giavaresi G, Martini L, Borsari V, Fini M. 2017. Osteoinductivity of nanostructured hydroxyapatite-functionalized gelatin modulated by human and endogenous mesenchymal stromal cells. J Biomed Mater Res Part A 2015:00A:000–000.

INTRODUCTION

The demand of new strategies for the induction of bone regeneration and repair is continuously increasing. Despite the high regenerative capacity of bone, many clinical situations require intervention, such as in the case of large bone defects caused by trauma, tumors or infection, but also in cases of spinal fusions and implant osteolysis.

The gold standard for the treatment of bone defects is autologous bone graft.[1,2] This represents the most effective treatment, but it is strongly limited by poor bone supply, donor site morbidity and patient-related bone quality.[3] Thus, it becomes necessary to develop new materials that could efficiently substitute bone grafts.

Suitable bone grafting biomaterials can be represented by polymers, ceramics, metals and composites. All of them possess advantages and disadvantages. In particular, scaffolds based on natural polymers are generally biodegradable (but sometimes with too high rates), biocompatible and bioactive, whereas their main drawbacks are low mechanical properties and low osteoinductivity.[2] Among biopolymers, relevant attention is addressed to gelatin, which is derived from the degradation of type-I collagen. Gelatin is by far cheaper than collagen and it is widely available as animal by-product (mainly bovine and porcine). It is also less antigenic than collagen[4] and susceptible to degradation by proteases.[5] The combination of gelatin with materials that have better mechanical performances could represent a strategy to improve the biological and mechanical properties of the resulting scaffolds. For this purpose, the enrichment of scaffold composition with calcium phosphates, such as biphasic calcium phosphate[6] or hydroxyapatite,[7,8] has the further advantage to provide scaffolds with the good bioactivity of

Correspondence to: Annapaola Parrilli; e-mail: annapaola.parrilli@ior.it

the inorganic phase. More complex composite scaffolds use combinations of several different materials in the attempt to improve their bone-regenerating properties,[9–11] or they can be carriers of bioactive molecules.[12–15]

In this context, we had previously developed biomimetic porous gelatin-nanocrystalline hydroxyapatite (HA) scaffolds with tailored properties.[16] The scaffolds were obtained by freeze-drying gelatin foams with different content of HA. These scaffolds, which were crosslinked with genipin to stabilize gelatin against dissolution in solution, displayed high connectivity and good porosity. The pore size distribution was modulated by HA content, in particular the mean pore size decreased as the inorganic phase increased. Mechanical strength improved on increasing HA content; however the material showed satisfying mechanical properties also with HA contents as low as 10 wt %. Most importantly, those gelatins showed a positive cellular response in terms of adhesion, proliferation and scaffold colonization of osteoblast-like cells. In addition, the presence of HA promoted their activity and differentiation. Based on the above results,[16] scaffolds containing 10 wt % HA (GEL-HA10) were chosen as the most promising in terms of porosity and cell colonization.

Therefore, the aim of this article was to investigate, both *in vitro* and *in vivo,* the osteoinductive properties of GEL-HA10 scaffolds, compared with those of scaffolds containing only gelatin (GEL) without the inorganic phase. The effect of scaffolds on osteogenic differentiation of human bone marrow mesenchymal stromal cells (hMSCs) was also investigated *in vitro*. The osteoinductive ability of scaffolds, with or without hMSCs supplementation, was then studied in a heterotopic model (subcutaneous implant in nude mice).

MATERIALS AND METHODS
Scaffolds preparation and characterization
The materials used for scaffold preparation were Type A gelatin (280 Bloom, Italgelatine SpA, Cuneo, Italy) from pig skin, and hydroxyapatite nanocrystals synthesized in aqueous medium as previously reported.[16] The following steps were utilized to prepare pure gelatin (GEL) scaffolds: a gelatin aqueous solution containing genipin (Wako, Japan) was exposed to constant mechanical stirring at 55°C, then allowed to gelify at the same temperature, washed in 0.1 M glycine aqueous solution, frozen in liquid N_2, and finally freeze dried. Scaffolds containing 10 wt % HA (GEL-HA10) were prepared by applying the same procedure to a gelatin solution containing HA. The methods details are reported in Panzavolta et al.[16] HA nanocrystals morphology was investigated using a TEM Philips CM100. A Philips XL-20 scanning electron microscope operating at 15 kV was used for the morphological and micro-structural characterizations of the scaffolds, which were sputter-coated with gold before being examined.

Osteogenic differentiation of human mesenchymal stromal cells
Cell cultures and media. hMSCs from a single donor were purchased from Cellular Engineering Technologies, Inc. (Coralville, IA) and cultured in Dulbecco's Modified Eagles Medium (DMEM, Sigma-Aldrich, St. Louis, MO), with 10%

fetal bovine serum (FBS, Lonza, Verviers, Belgium), 100 U/ml penicillin, 100 µg/ml streptomycin (Gibco, Life Technologies, Carlsbad, CA) and 5 µg/ml plasmocin (Invivogen, San Diego, CA). GEL and GEL-HA10 samples were prepared as previously described.[16] Samples were 5 mm in diameter and 2 mm in thickness (volume ~40 mm^3), as shown in Figure 1a. Samples (GEL $n = 24$ and GEL-HA10 $n = 24$) were pre-soaked in medium and any surplus was discarded before cell seeding. Cells up to passage 5 were used for all experiments. Cells were seeded (7.5×10^4) on the top of GEL and GEL-HA10 samples in osteogenic medium, that is, growth medium with the addition of 7 mM β-glycerophosphate, 50 µg/ml ascorbic acid 2-phosphate and 0.1 mM dexamethasone (Sigma-Aldrich). A small seeding volume (15 µl) was used to allow cells to be absorbed and not released by the materials. Osteogenic medium (500 µl) was added 2 hours after cell seeding. Cultures were maintained at 37°C, 5% CO_2 for 1 and 3 weeks, and the medium was replaced every two days. Monolayer cultures of hMSCs in osteogenic medium were used as controls (CRL).

Analysis of cell proliferation. Cell proliferation was assessed by alamarBlue (ABD Serotec, Oxford, UK) assay, following the manufacturer's instruction on $3 + 3$ (1 and 3 weeks) samples for each group (CRL, GEL and GEL-HA10 groups). Briefly, cells were incubated with a solution of 10% alamarBlue in medium for 3.5 hours at 37°C. Afterwards, the optical density of the supernatants was measured at 570 and 625 nm. The percentage of alamarBlue reduction was calculated with the following formula: %RED $= [A_{LW} - (A_{HW} \times R_0)] \times 100$.

A_{LW}: difference between sample absorbance and alamarBlue absorbance in media (blank) at 570 nm; A_{HW}: difference between sample absorbance and blank absorbance at 625 nm; R_0 is a correction factor calculated as AO_{LW}/AO_{HW}. AO_{LW}: difference between blank absorbance and medium absorbance at 570 nm. AO_{HW}: difference between blank absorbance and medium absorbance at 625 nm.

Alkaline phosphatase activity. Cells, derived from $3 + 3$ (1 and 3 weeks) samples for each group, were lysed with 0.1% sodium dodecyl sulfate (SDS) in dH_2O, followed by the addition of 20 mM p-nitrophenyl phosphate in glycin buffer (glycin 0.1 M, $MgCl_2$ 1 mM, $ZnCl_2$ 1 mM, pH 10.4 in dH_2O). The absorbance of the solution was measured at 405 nm (iMark™ Microplate Absorbance Reader, Bio-Rad, Hercules, CA) and the concentration of the product, 4-nitrophenol, was calculated referring to a standard curve. All chemicals were purchased from Sigma-Aldrich. Results were normalized to total DNA content in cell lysates that was quantified with the Quant-iT PicoGreen dsDNA Assay Kit (Invitrogen, Life Technologies) following the manufacturer's instructions.

Gene expression. Total RNA, derived from $3 + 3$ (1 and 3 weeks) samples for each group, was extracted with a phenol-chloroform method using TRIzol Reagent (Invitrogen, Life Technologies) and reverse transcribed using the SuperScript VILO cDNA Synthesis Kit (Invitrogen, Life Technologies),
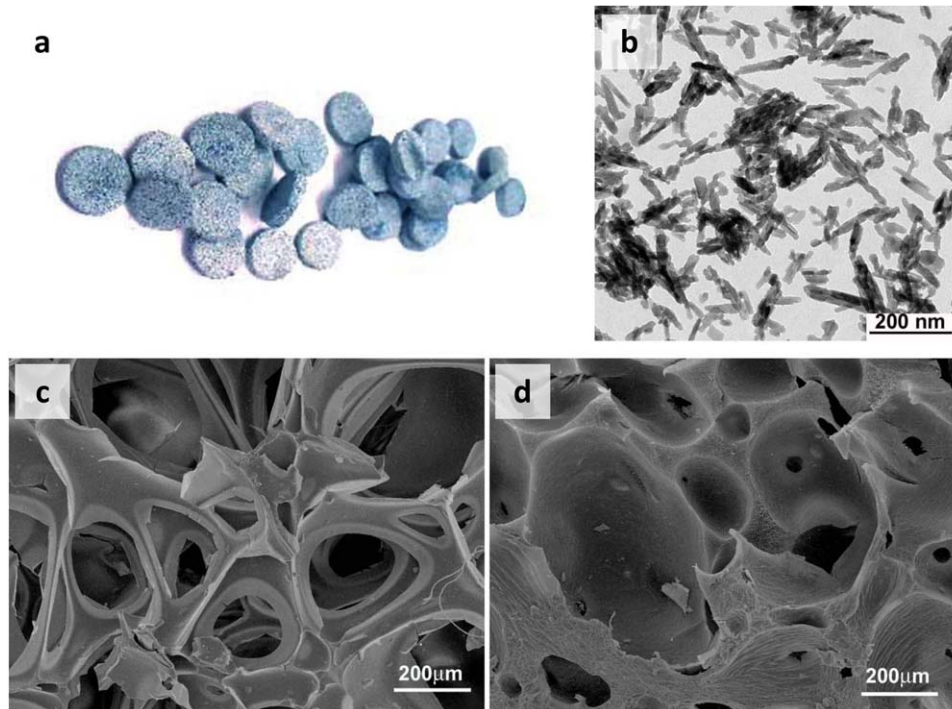
FIGURE 1. (a) Macroscopic pictures of freeze-dried gelatin foams crosslinked with genipin. (b) TEM image of hydroxyapatite nanocrystals utilized to prepare GEL-HA10 scaffolds. The crystals exhibit a rod-like shape and mean dimensions smaller than 100 nm. (c and d) Cross-sectional SEM micrographs of GEL (c) and GEL-HA10 (d) scaffolds, showing the morphology of pores.

following the manufacturer instructions. Relative expression was assessed for the following genes: *RUNX2*, *SP7*, *ALPL*, *COL1A1*, *VEGFA*, and *BGLAP*, with *GAPDH* as reference (see Table I for detailed primer reference). Semi-quantitative polymerase chain reaction (PCR) analysis was performed in a LightCycler 2.0 Instrument (Roche Diagnostics GmbH, Manheim, Germany) using QuantiTect SYBR Green PCR Kit (Qiagen, Hilden, Germany). The amplification protocol included an initial denaturation at 94°C for 15 min, 35 cycles of amplification (94°C for 15″, 55°C–56°C for 20″ and 72°C for 20″), and a melting curve analysis. The threshold cycle was determined for each sample and relative gene expression was calculated using the $2^{-\Delta\Delta Ct}$ method[17] with control samples at 1 week as calibrators.

Histological analyses on constructs. Constructs cultured for 1 and 3 weeks (GEL $n = 3 + 3$ and GEL-HA10 $n = 3 + 3$) were fixed in 10% neutral buffered formalin, decalcified in 14% EDTA, dehydrated in increasing concentrations of alcohol solutions, embedded in paraffin, and sectioned (Micron HM 340E, Microm International GmbH, Germany). One cross-sectional cut was made at an intermediate level of the sample, and 5 μm-thick sections were cut and stained with Hematoxylin and Eosin (H&E). Sections were evaluated for the presence of cells and extracellular matrix at different magnifications. Images were captured using the qualitative, semi-automated light microscope Olympus BX51 (BX51, Olympus Optical Co. Europe GmbH, Germany) and the image analysis system cellSens (Olympus).

In vivo ectopic bone formation

Animal model. *In vivo* experiments were conducted in agreement with the European and Italian Law on animal studies. The protocol was approved by the Ethical Committee of the Rizzoli Orthopedic Institute and authorized by the Italian Ministry of Health.

Twenty-six athymic nude male mice (Harlan Laboratories Srl, Udine, Italy) aged 6 weeks, 25 ± 5 g b.w., were housed in groups (according with Directive 2010/63 EU and with Commission Recommendation 2007/526/EC) in plastic cages (Techniplast S.p.A, Buguggiate, Italy) at a controlled room temperature of $22°C \pm 1°C$ and relative humidity of $50\% \pm 5\%$, with controlled ventilation. Mice were fed with a standard pellet diet (Mucedola S.r.l., Settimo Milanese, Italy) and water *ad libitum*.

Surgery was performed under general anesthesia, induced by a combination of 100 mg/kg ketamine (Imalgene 1000, Merial Italia S.p.A, Milan, Italy) and 5 mg/kg xylazine (Rompun, Bayer Italia S.p.A., Milan, Italy). In the postoperative period, 0.5 ml of glucose solution was administered and mice were maintained in single cages in a confined room at $23°C \pm 1°C$ until complete recovery. Animals were checked daily to evaluate their general clinical conditions. No complications or reactions in the implant site were registered. At the end of the experimental time (8 weeks), mice were euthanized under general anesthesia with i.c. injection of 0.5 ml Tanax (Hoechst Roussel Vet GmbH, Wiesbaden, Germany).

***In vivo* experimental setup.** Commercial hMSCs were purchased from Cellular Engineering Technologies, Inc. and

TABLE I. Real-Time PCR Primers Specifications

Human Primers

Gene	Forward Primer	Reverse Primer	Ann T	Notes
GAPDH	TGGTATCGTGGAAGGACTCA	GCAGGGATGATGTTCTGGA	56°C	Custom primers Life Technologies
RUNX2	QuantiTect Primer Assay Hs_RUNX2_1_SG		55°C	QuantiTect Primer Assay Qiagen
SP7	QuantiTect Primer Assay (Qiagen) Hs_SP7_1_SG		55°C	QuantiTect Primer Assay Qiagen
COL1A1	QuantiTect Primer Assay Hs_COL1A1_1_SG		55°C	QuantiTect Primer Assay Qiagen
ALPL	QuantiTect Primer Assay Hs_ALPL_1_SG		55°C	QuantiTect Primer Assay Qiagen
BGLAP	ACACTCCTCGCCCTATTG	GATGTGGTCAGCCAACTC	55°C	Custom primers Life Technologies
VEGFA	QuantiTect Primer Assay (Qiagen) Hs_VEGFA_6_SG		55°C	QuantiTect Primer Assay Qiagen

Mouse Primers

Gene	Forward Primer	Reverse Primer	Ann T	Notes
Gapdh	AATGGTGAAGGTCGGTGTG	GTGGAGTCATACTGGAACATGTAG	60°C	PrimeTime Assay IDT
Alpl	CAAGGACATCGCATATCAGCTA	GCCTTCTCATCCAGTTCGTAT	60°C	PrimeTime Assay IDT
Col1a1	CGCAAAGAGTCTACATGTCTAGG	CATTGTGTATGCAGCTGACTTC	60°C	PrimeTime Assay IDT
Bglap	AGCAGAGTGAGCAGAAAGATG	GAACAGACAAGTCCCACACAG	60°C	PrimeTime Assay IDT

used at their fifth passage, like for the *in vitro* studies described above. Cells were seeded on materials 24 hours before implantation at a density of 10^6 cells/implant. Non-seeded or hMSC-seeded GEL or GEL-HA10 samples were implanted into subcutaneous left or right side pockets formed in the dorsal surface of the mice. Two implants were made on each mouse. Experimental groups included: GEL ($n = 11$); GEL + hMSCs ($n = 11$); GEL-HA10 ($n = 15$); GEL-HA10 + hMSCs ($n = 15$). After euthanasia, implants were retrieved and cut into half: one for histology and one for gene expression analysis.

In vivo micro-computed tomography (micro-CT). At 8 weeks, the process of ectopic bone formation was monitored by *in vivo* microtomography (Skyscan 1176, Bruker microCT, Kontich, Belgium) applying a source voltage of 50 kV and a source current of 500 µA on 20 animals randomly chosen (10 animals each material). The nominal resolution used for images was set at 9 µm (pixel size). The images (2672 × 4000 pixels) were then reconstructed with NRecon program (Bruker microCT) to obtain micro-CT sections (4000 × 4000 pixels, maintaining the relative pixel size = 9 µm). In addition to the specific alignment, beam hardening and reduction of ring artifacts were used as correction factors in the reconstruction process. The presence of mineralized tissue in the micro-CT section was analyzed and expressed both qualitatively and quantitatively using CTAn software (Bruker microCT) after applying a global threshold determined by the differences in pixel grey level between soft and hard tissues. The threshold of the rat vertebrae bone was taken as reference. In addition, in order to

compare the results longitudinally, 2 animals implanted with GEL scaffolds and 5 animals implanted with GEL-HA10 scaffolds were scanned at 0 weeks and analyzed using the same procedure described above.

Histological analyses on implants. Retrieved implants were fixed in 10% neutral buffered formalin for 24 hours and washed in dH$_2$O. Samples were decalcified in a mixture of formic and hydrochloric acids for 24 hours, then dehydrated in 70%–100% ethanol (Carlo Erba Reagents, Milan, Italy), cleared in xylene (Carlo Erba Reagents) and paraffin embedded. Five micrometer-thick sections were cut transversally with the microtome Micron HM 340E and stained with H&E. Images were captured using the digital scanner Aperio (Aperio CS2, Leica Biosystems, Buffalo Grove, IL) and analyzed with the Aperio ImageScope software (Aperio CS2, Leica Biosystems).

Gene expression analysis. One half of each implant was cleaned from the surrounding tissue and immediately submerged in RNA*later* Stabilization Solution (Ambion, Life Technologies). After an overnight incubation at 4°C to allow the complete penetration of the solution, samples were stored at −80°C until further analyses. Samples were homogenized using a cryogenic mill (6770 Freezer/Mill, SPEX SamplePrep, Metuchen, NJ). Total RNA was extracted with a phenol-chloroform method using TRIzol reagent (Life Technologies) and processed as described above for *in vitro* samples. Relative expression was assessed differentially for the following human or mouse genes: *COL1A1*, *BGLAP*, and *ALPL*, with *GAPDH* as reference (refer to Table I for primer
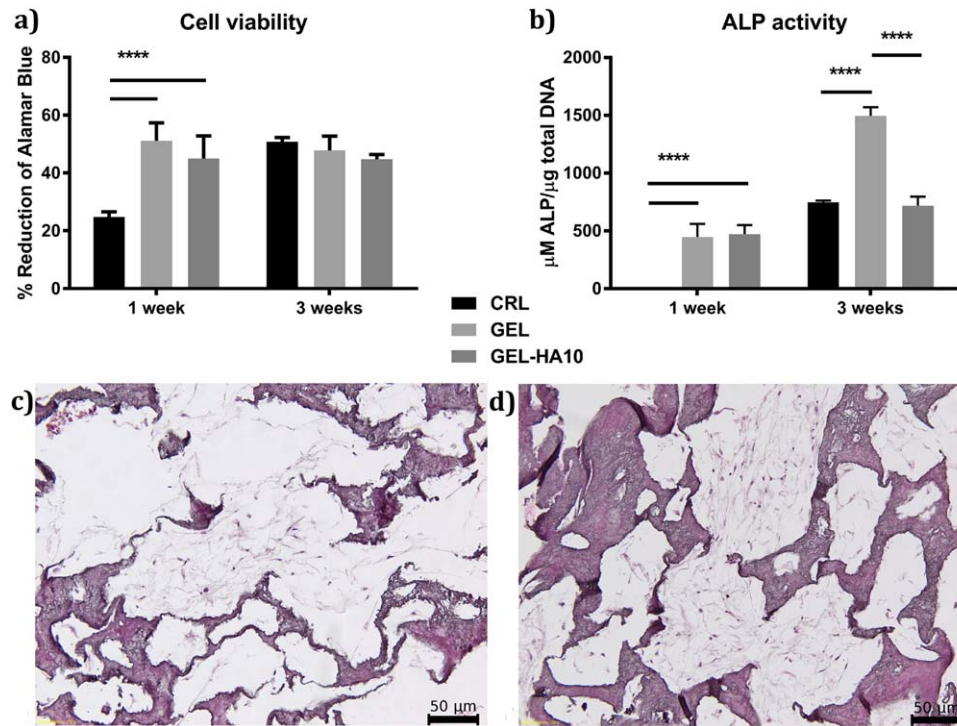
FIGURE 2. *In vitro* analysis of hMSC differentiation on GEL and GEL-HA10 scaffolds. (a) Analysis of cell viability with alamarBlue assay; (b) Analysis of alkaline phosphatase (ALP) activity, normalized to total DNA content. No ALP activity was detectable in CRL samples at 1 week. Results are reported as mean $\pm$ SD. ****$p < 0.0005$; Representative histological images of (c) GEL and (d) GEL-HA10 scaffolds stained with H&E at 3 weeks showing cell growth.

details). Results are reported as $2^{-\Delta Ct}$. Fold changes in gene expression of GEL-HA10 versus GEL samples were calculated as the ratio of their $2^{-\Delta Ct}$ values.

Statistical analysis

Statistical analysis was performed using IBM SPSS Statistics v.23. A two-way ANOVA with Holm-Sidak multiple comparisons was used to test the main effects of fixed factors "scaffold" (GEL and GEL-HA10) and "condition" (experimental times—1 and 3 weeks—for *in vitro* study and hMSC—scaffold seeded or unseeded—for *in vivo*) experiments. Interactions on data. χ^2 tests were used to calculate the proportion of *in vivo* GEL-HA10 samples positive for gene expression compared to GEL samples, and the proportion of expressed murine genes in engineered scaffolds in comparison to those expressed in cell-free scaffolds GEL or in comparison with human genes expressed in engineered scaffolds. Unpaired *t* tests were used to compare the expression of human genes between GEL and GEL-HA10 samples.

RESULTS

The synthesized hydroxyapatite nanocrystals utilized to prepare GEL-HA10 scaffolds (see Fig.1a for macroscopic appearance of scaffolds) exhibit a rod-like shape and mean dimensions smaller than 100 nm (Fig.1b). The presence of the inorganic phase does not appreciably affect the porosity of the scaffolds, which is similar to that of GEL scaffolds.[16] Typical cross-sectional scanning electron microscopy images are reported in Fig. 1c,d.

Osteogenic differentiation of human mesenchymal stromal cells

Both GEL and GEL-HA10 sustained the proliferation of hMSCs that was higher at 1 week compared with CRL, $p < 0.0005$ (Fig. 2a). ALP activity was undetectable in CRL samples at 1 week. Moreover, ALP increased at 3 weeks in GEL samples compared with CRL, $p < 0.0005$, while GEL-HA10 samples showed values similar to controls (Fig. 2b).

Histological analysis on constructs revealed that hMSCs could easily colonize the scaffolds and produce extracellular matrix (Fig. 2c,d), especially GEL-HA10 samples at 3 weeks (Fig. 2d). The presence of cells was observed in the whole thickness of the scaffolds, thus confirming their optimal properties for cell growth and colonization.

Results of gene expression analysis revealed that *SP7*, *BGLAP*, and *VEGFA* levels were higher in GEL-HA10 samples compared to CRL and GEL at 3 weeks. GEL-HA10 samples also showed an early upregulation of *SP7* and *BGLAP*. *RUNX2* expression was downregulated at 1 week in GEL and GEL-HA10 compared to CRL. *COL1A1* and *RUNX2* showed a similar expression profile, even though only GEL samples were significantly different from CRL for *COL1A1*. *ALPL* expression was also downregulated in GEL samples at 3 weeks (Fig. 3).

In vivo ectopic bone formation

In vivo, micro-CT showed the osteoinductive potential of both GEL and GEL-HA10 scaffolds. However, the materials seeded with hMSC showed osteoinductive characteristics
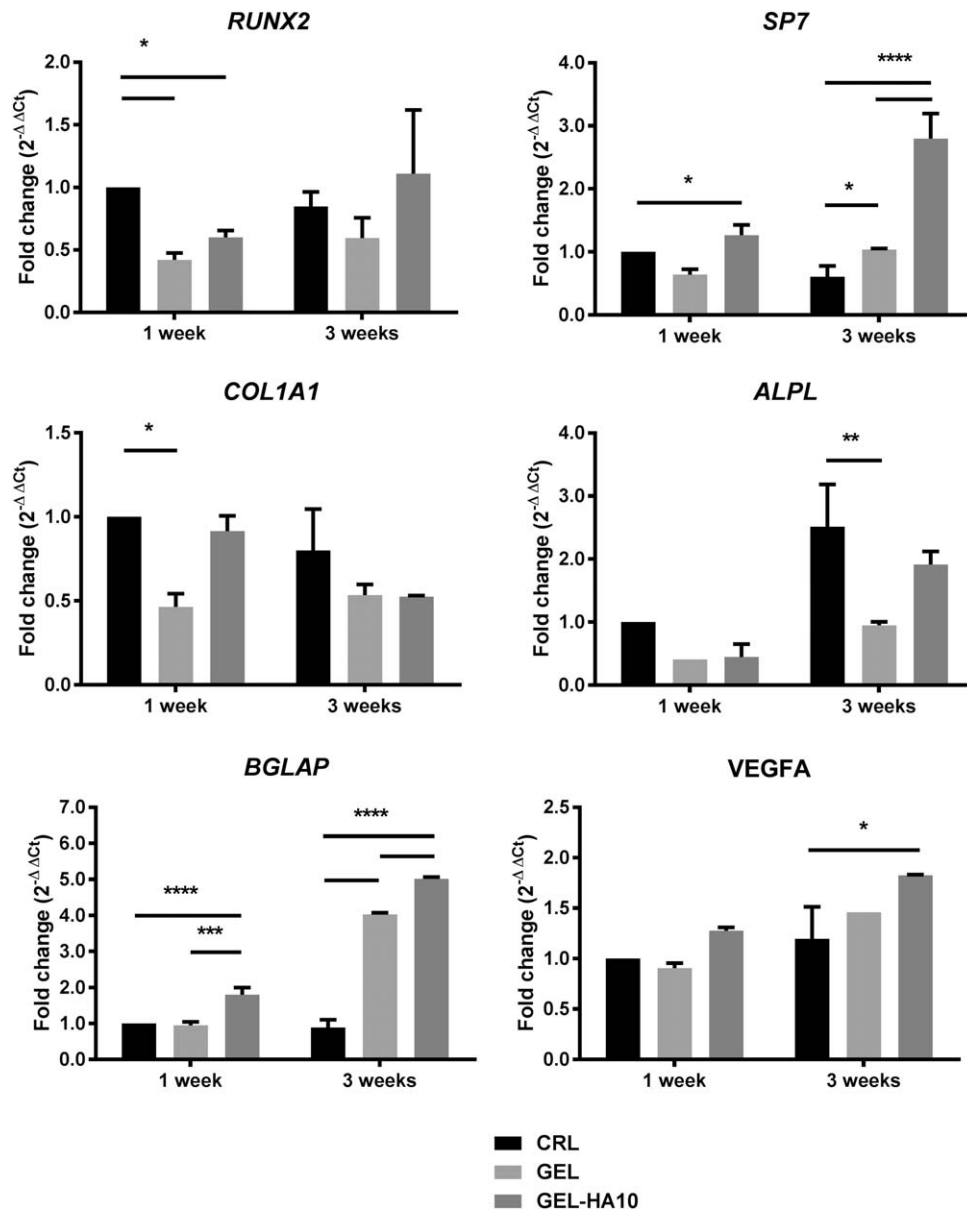
FIGURE 3. Relative gene expression of osteogenic markers assessed after 1 and 3 weeks of osteogenic differentiation of hMSCs on GEL and GEL-HA10 scaffolds. Fold changes were calculated as $2^{-\Delta\Delta Ct}$ using the CRL sample (monolayer) at 1 week as calibrator and *GAPDH* as reference gene. Statistical differences are reported as *$p < 0.05$; **$p < 0.01$; ***$p < 0.001$; ****$p < 0.0001$.

only with the presence of HA. The presence of mineralized tissue in the micro-CT section and the scaffolds osteoinductive capability were determined by the differences in pixel grey level. Mineralized areas presented lighter grey colored pixels (Fig. 4). This ectopic bone formation was analyzed and expressed both as proportion of *in vivo* samples showing lighter grey level areas in correspondence of the implants, and as volume in mm^3 (Table II and Fig. 4). At 8 weeks, results showed that both cell-free GEL and GEL-HA10 samples had mineralized. In groups with the presence of hMSC, mineralized tissue was detected in only one case out of 10 (10%) of GEL samples, while GEL-HA10 continued to have a high percentage of samples with ectopic bone formation (90%, $p < 0.0005$), even though the quantified

volume of mineralized tissue was significantly lower than in cell-free scaffolds (Fig. 4).

Histological analysis of explants revealed no connective tissue capsule around the implanted scaffolds. GEL implants showed differences between hMSC-seeded or cell-free scaffolds. In GEL scaffolds, host cells were found mainly on superficial layers while the center of the scaffold presented empty spaces. Mineralized tissue with bone lacunae was found mainly and almost exclusively on the scaffold borders (Fig. 5a,e). In contrast, GEL + hMSC scaffolds showed the production of a connective tissue without the presence of mineralization nuclei (Fig. 5b,f). Besides, no lacunae were detected and cells were located mostly on the surfaces of the extracellular matrix. Similarly, in GEL-HA10 samples
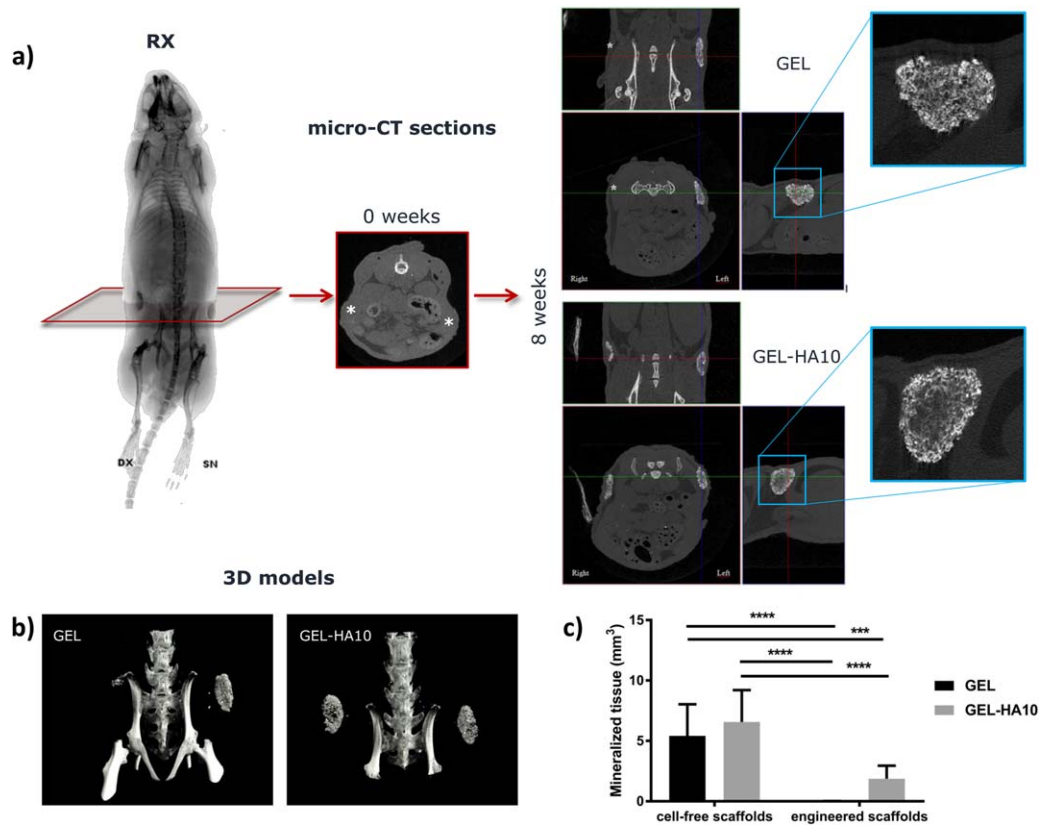
FIGURE 4. Micro-CT analysis. (a) Example of a radiograph (RX) and *in vivo* micro-CT sections of samples with subcutaneous GEL implantation just after surgery ($t = 0$ weeks) and after 8 weeks ($t = 8$ weeks). Blue panels show detailed pictures corresponding to the implanted scaffolds. Asterisks indicate the un-mineralized implanted scaffolds; (b) 3D models of implanted GEL and GEL-HA10 at 8 weeks; (c) Histogram of the detected mineralized tissue (***$p < 0.001$; ****$p < 0.0001$).

mineralized tissue with bone lacunae was found mainly at the scaffold borders. However, a higher presence of blood vessels was detected (Fig. 5c,g). GEL-HA10 + hMSC showed mineralized tissue as well (unlike the GEL + hMSC), with the presence of multinucleated cells located especially close to the scaffold borders and on the external layers (Fig. 5d,h).

RNA was successfully extracted and, after reverse transcription, the analysis of the housekeeping gene *GAPDH* in quantitative PCR (qPCR) revealed satisfactory Ct values in every sample. Gene expression of osteogenic markers varied among different samples both as presence/absence and as levels. Table III shows the proportion of samples showing the expression of a specific gene, while Figure 6 reports gene expression levels in positive samples. In these positive samples, qPCR analysis showed that the expression of murine

Col1a1 and *Alpl* was enhanced by the presence of hMSCs (Fig. 6). However, the presence of HA had almost no effect on murine gene expression, except for a decrease in *Col1a1* expression. Regarding the expression of human genes, the different composition of scaffolds resulted in a different pattern of gene expression: indeed, while no difference was revealed in *COL1A1* levels, the expression of *ALPL* and *BGLAP* increased in GEL-HA10 compared to GEL samples, with a mean fold increase of 8.88 and 120.10, respectively ($p < 0.05$, Fig. 6).

DISCUSSION

Bone tissue engineering is aimed at treating diseases that involve impaired bone healing and requires the development of new effective biomaterials. Gelatin-based biomaterials

TABLE II. Proportion of *In Vivo* Samples with the Presence of Mineralized Tissue and New Bone Formation in mm^3 Detected in Micro-Ct Sections. χ^2 Test Evaluated the Differences Among Mineralized Tissue Amount in Samples

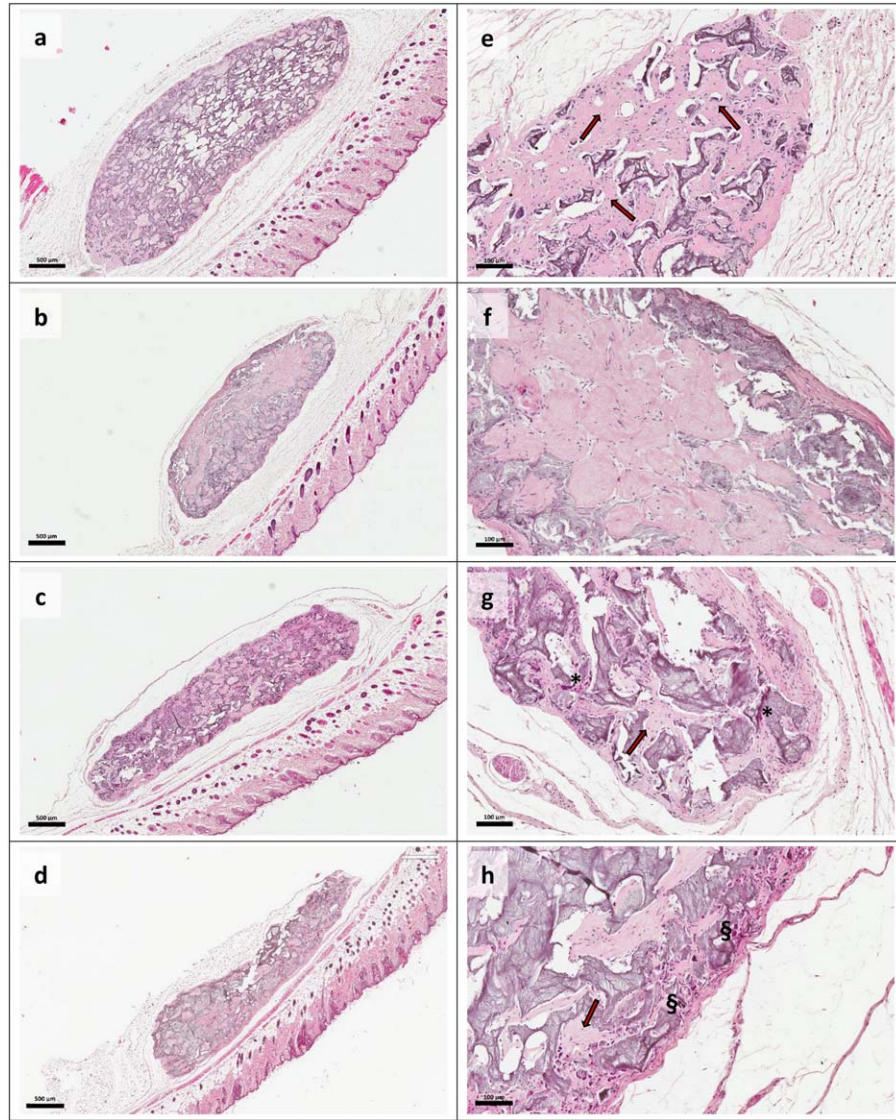|	0 weeks			8 weeks		
	GEL	GEL-HA10	p	GEL	GEL-HA10	p
Cell-free scaffolds	0/2 (0%)	0/5 (0%)	ns	10/10 (100%) 5.41 ± 2.61 mm^3	10/10 (100%) 6.57 ± 2.64 mm^3	ns
Engineered scaffolds (hMSC)	0/2 (0%)	0/5 (0%)	ns	1/10 (10%) 0.01 ± 0.01 mm^3	9/10 (90%) 1.86 ± 1.08 mm^3	0.0005
Engineered versus cell-free scaffolds	ns	ns		0.0005	ns	

FIGURE 5. Representative histological sections of GEL and GEL-HA10 scaffolds, stained with Hematoxylin and Eosin. (a–e) cell-free GEL implants; (b–f) hMSC-seeded GEL implants; (c–g) cell-free GEL-HA10 implants; (d–h) hMSC-seeded GEL-HA10 implants. Scale bars (500 μm in a–d and 100 μm in e–h) are reported on the bottom-left corner of each image. Arrows indicate lacunae, asterisks indicate the presence of blood vessels inside the scaffolds, while § symbols indicate multinuclear cells.

possess promising properties in terms of biocompatibility, bioactivity and degradability, suggesting that composite or functionalized gelatin scaffolds could display improved

activity and mechanical properties. In this regard, our group had previously developed biomimetic gelatin-nanocrystalline HA porous scaffolds that showed promising results in terms

TABLE III. Proportion of *In Vivo* Samples Positive for Gene Expression. χ^2 **Test Evaluated the Differences Among Percentages of Gene Expression in Samples**

|	COL1A1			ALPL			BGLAP		
	GEL	GEL-HA10	*p*	GEL	GEL-HA10	*p*	GEL	GEL-HA10	*p*
a) Murine genes in cell-free scaffolds	10/10 (100%)	15/15 (100%)	ns	8/10 (80%)	8/15 (53%)	*ns*	6/10 (60%)	14/15 (93%)	ns
b) Murine genes in engineered scaffolds	11/11 (100%)	15/15 (100%)	ns	4/11 (36%)	10/15 (67%)	*ns*	10/11 (91%)	14/15 (93%)	ns
c) human genes in engineered scaffolds	11/11 (100%)	14/15 (93%)	ns	6/11 (55%)	10/15 (67%)	*ns*	4/11 (36%)	5/15 (33%)	ns
b) versus a), *p*	ns	ns		0.056	ns		ns	ns	
c) versus b), *p*	ns	ns		ns	ns		ns	0.0008	
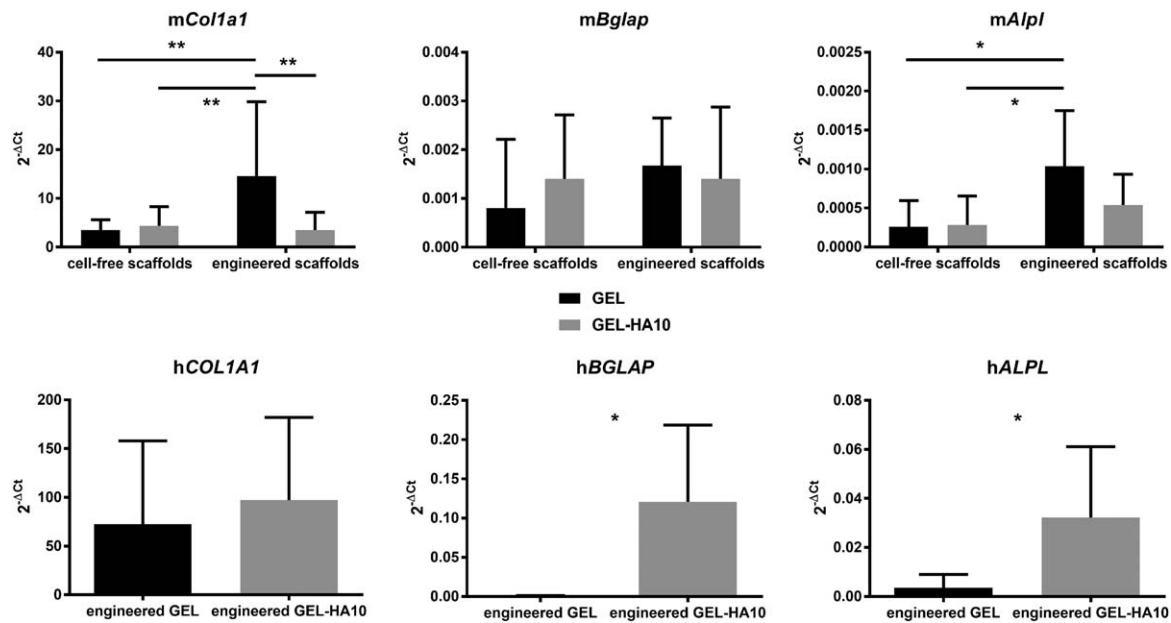
FIGURE 6. Relative gene expression of osteogenic markers assessed after 8 weeks of osteoinduction of GEL and GEL-HA10 scaffolds, with or without hMSCs supplementation, in a heterotopic model (subcutaneous implant in nude mice). Fold changes were calculated as $2^{-\Delta Ct}$ using *GAPDH* as reference gene. The levels of murine or human gene expression was assessed differentially, using species-specific primers. Upper row: expression of murine genes. Lower row: expression of human genes. Statistical differences are reported as *$p < 0.05$; **$p < 0.01$.

of enhanced osteoblast-like cells and extracellular matrix mineralization processes activation.[16] On this basis, we decided to test the osteoinductive properties of these scaffolds both *in vitro* and in an *in vivo* ectopic bone formation model with subcutaneous implantation in nude mice. The results demonstrated that the material enhanced osteogenic differentiation of hMSC *in vitro* and it was *per se* osteoinductive *in vivo*; in fact, even more mineralized tissue was detected in the absence of pre-implanted hMSC.

GEL and GEL-HA10 scaffold sustained the differentiation of hMSC *in vitro*, with increased ALP activity and higher expression of bone specific genes such as *BGLAP* and *SP7*. Moreover, the upregulation of *VEGFA* in GEL-HA10 samples may be beneficial for osteogenesis/angiogenesis coupling, critical for a successful bone regeneration.[18,19]

The expression of murine bone-specific genes *in vivo* did not differ between scaffolds, with an upregulation of *Col1a1* and *Alpl* in the presence of pre-implanted hMSC. In a different manner, differential gene expression analysis revealed that the presence of nanocrystalline HA induced the upregulation of bone-specific genes in human cells. Even if the difference between murine and human cells in response to HA may reflect just the difference between naïve and monolayer-expanded cells, our opinion is that the species-specific response play a prominent role. In fact, murine cells were able to generate a mineralized matrix both in GEL and GEL-HA10 scaffolds when not engineered with hMSCs. In addition, no statistical difference was observed in the volume of the mineralized tissue formed between the two materials independently from the presence of HA. The difference in response to HA between murine and human cells is a noteworthy result. Indeed, to our knowledge, this is the

first study that examined the different response of murine and human cells and showed the persistence of human cells after 8 weeks *in vivo*. Interestingly, nearly no mature mineralized tissue was found at 8 weeks in GEL + hMSC samples, whereas micro-CT scans revealed mineralization in all other groups. Generally, the presence of pre-implanted hMSCs in the scaffolds resulted in an inhibition of mineralization. This result was unexpected because it contradicts some previous result found in literature.[20,21] Like our findings, Miramond et al. found no osteoinduction when hMSCs were seeded in bioceramic scaffolds implanted subcutaneously in a murine model.[22] The authors hypothesized that high cell seeding density (20 million cells/g of material) formed a sort of dense matrix gel, thus preventing both nutrients from reaching the cells and therefore hampering the recruitment of endogenous cells. Unlike the article by Miramond, our study showed a recruitment of host cells, as demonstrated by murine-specific RNA detected in explanted samples. We excluded issues in osteogenic differentiation of murine cells because their differentiation level was comparable to non-seeded scaffolds, as shown from gene expression analysis (Fig. 6). It is possible that the presence of hMSC allowed the recruitment of a lower number of endogenous cells despite their differentiation potential remained the same. The presence of hMSC could inhibit the process of mineralization of host cells probably reducing the bioavailability of minerals to be deposited in the extracellular matrix or interfering with the mineralization-initiating processes. As demonstrated by *in vivo* outcomes, we noted that while host cells showed comparable expression levels of osteogenic markers between GEL and GEL-HA10 samples, hMSCs were induced to osteogenic differentiation by the presence of HA, if

compared to GEL samples. In our opinion, the presence of mineralized tissue in GEL-HA10 could be predominantly due to the osteogenic activity of hMSC and the presence of HA. Even though this hypothesis should be substantiated by additional tests, in our study we could analyze differences in the response of murine (host) and human (pre-implanted) cells to HA, observing an upregulation of osteogenic markers only in hMSC. It is recognized that the process of osteoinduction differs from species to species, and the scaffolds implanted in heterotopic models show different results in different animal models.[23-25]

In summary, both GEL and GEL-HA10 scaffolds showed promising osteoinductive properties in a subcutaneous bone formation model when implanted without hMSCs. The use of pre-implanted hMSC abolished or reduced mineralization of GEL and GEL-HA10 scaffold, therefore it is not clear whether the use of hMSC in a clinical setting will be beneficial for the patient. Ectopic bone formation and undifferentiated human cells pre-seeding may not represent the best *in vivo* model for the evaluation of osteoinduction because it does not give information about interaction or synergy between all kinds of involved cells and the material. However, we could observe a different response to the presence of HA, which stimulated osteogenic differentiation of human cells only. Therefore, the model used and the differential analysis between murine and human cells allow a more accurate prediction of the possible reaction of endogenous hMSC that could be recruited if the scaffolds are used in patients, increasing the clinical relevance of this study. We suggest that our scaffolds may be tested for clinical use in confined critical defects.

DISCLOSURES

The authors declare no conflict of interest.

BIBLIOGRAPHY

1. Oryan A, Alidadi S, Moshiri A, Maffulli N. Bone regenerative medicine: Classic options, novel strategies, and future directions. J Orthop Surg Res 2014;9:18.
2. García-Gareta E, Coathup MJ, Blunn GW. Osteoinduction of bone grafting materials for bone repair and regeneration. Bone 2015;81:112–121.
3. Sen MK, Miclau T. Autologous iliac crest bone graft: Should it still be the gold standard for treating nonunions? Injury 2007;38:S75–S80.
4. Su K, Wang C. Recent advances in the use of gelatin in biomedical research. Biotechnol Lett 2015;37:2139–2145.
5. CB. Gelatin In: Wiley Encyclopedia of food science and technology, 2nd ed. In: Francis, F.J, John, editor. New York, NY: Wiley & Sons; 1999. p 1183–1188.
6. Nguyen TB, Min YK, Lee BT. Nanoparticle biphasic calcium phosphate loading on gelatin-pectin scaffold for improved bone regeneration. Tissue Eng Part A 2015;21:1376–1387.
7. Chiu CK, Ferreira J, Luo TJ, Geng H, Lin FC, Ko CC. Direct scaffolding of biomimetic hydroxyapatite-gelatin nanocomposites using aminosilane cross-linker for bone regeneration. J Mater Sci Mater Med 2012;23:2115–2126.
8. Sadat-Shojai M, Khorasani MT, Jamshidi A. 3-Dimensional cell-laden nano-hydroxyapatite/protein hydrogels for bone regeneration applications. Mater Sci Eng C Mater Biol Appl 2015;49:835–843.
9. Ferreira JR, Padilla R, Urkasemsin G, Yoon K, Goeckner K, Hu WS, Ko CC. Titanium-enriched hydroxyapatite-gelatin scaffolds with osteogenically differentiated progenitor cell aggregates for calvaria bone regeneration. Tissue Eng Part A 2013;19:1803–1816.
10. Martínez-Vázquez FJ, Cabañas MV, Paris JL, Lozano D, Vallet-Regí M. Fabrication of novel Si-doped hydroxyapatite/gelatine scaffolds by rapid prototyping for drug delivery and bone regeneration. Acta Biomater 2015;15:200–209.
11. Sharma C, Dinda AK, Potdar PD, Chou CF, Mishra NC. Fabrication and characterization of novel nano-biocomposite scaffold of chitosan-gelatin-alginate-hydroxyapatite for bone tissue engineering. Mater Sci Eng C Mater Biol Appl 2016;64:416–427.
12. Hokugo A, Saito T, Li A, Sato K, Tabata Y, Jarrahy R. Stimulation of bone regeneration following the controlled release of water-insoluble oxysterol from biodegradable hydrogel. Biomaterials 2014;35:5565–5571.
13. Omata K, Matsuno T, Asano K, Hashimoto Y, Tabata Y, Satoh T. Enhanced bone regeneration by gelatin-β-tricalcium phosphate composites enabling controlled release of bFGF. J Tissue Eng Regen Med 2014;8:604–611.
14. Lee JH, Lee YJ, Cho HJ, Kim DW, Shin H. The incorporation of bFGF mediated by heparin into PCL/gelatin composite fiber meshes for guided bone regeneration. Drug Deliv Transl Res 2015;5:146–159.
15. Teotia AK, Gupta A, Raina DB, Lidgren L, Kumar A. Gelatin-modified bone substitute with bioactive molecules enhance cellular interactions and bone regeneration. ACS Appl Mater Interfaces 2016;8:10775–10787.
16. Panzavolta S, Torricelli P, Amadori S, Parrilli A, Rubini K, Della Bella E, Fini M, Bigi A. 3D interconnected porous biomimetic scaffolds: In vitro cell response. J Biomed Mater Res A 2013;101:3560–3570.
17. Livak KJ, Schmittgen TD. Analysis of relative gene expression data using real-time quantitative PCR and the 2(-Delta Delta C(T)) Method. Methods 2001;25:402–408.
18. Kanczler JM, Oreffo RO. Osteogenesis and angiogenesis: The potential for engineering bone. Eur Cell Mater 2008;15:100–114.
19. Kusumbe AP, Ramasamy SK, Adams RH. Coupling of angiogenesis and osteogenesis by a specific vessel subtype in bone. Nature 2014;507:323–328.
20. Kadiyala S, Jaiswal N, Bruder SP. Culture-expanded, bone marrow-derived mesenchymal stem cells can regenerate a critical-sized segmental bone defect. Tissue Eng 1997;3:173–185.
21. Arinzeh TL, Tran T, Mcalary J, Daculsi G. A comparative study of biphasic calcium phosphate ceramics for human mesenchymal stem cell-induced bone formation. Biomaterials 2005;26:3631–3638.
22. Miramond T, Corre P, Borget P, Moreau F, Guicheux J, Daculsi G, Weiss P. Osteoinduction of biphasic calcium phosphate scaffolds in a nude mouse model. J Biomater Appl 2014;29:595–604.
23. Yuan H, van Blitterswijk CA, de Groot K, de Bruijn JD. Cross-species comparison of ectopic bone formation in biphasic calcium phosphate (BCP) and hydroxyapatite (HA) scaffolds. Tissue Eng 2006;12:1607–1615.
24. Akiyama N, Takemoto M, Fujibayashi S, Neo M, Hirano M, Nakamura T. Difference between dogs and rats with regard to osteoclast-like cells in calcium-deficient hydroxyapatite-induced osteoinduction. J Biomed Mater Res A 2011;96:402–412.
25. Tsukanaka M, Fujibayashi S, Otsuki B, Takemoto M, Matsuda S. Osteoinductive potential of highly purified porous β-TCP in mice. J Mater Sci Mater Med 2015;26:132.